Jurnal Sains Nuklear Malaysia, 2025, 37(No.1): 33 – 49
ISSN: 2232-0946

PREDICTION OF RTP FUEL SOURCE TERM AND DECAY HEAT IN SURROUNDING MATERIALS

Mohamad Hairie Rabir*, Mark Dennis Usang, Muhammad Khairul Ariff Mustafa, Julia Abdul Karim and Mohamad Amirudin Mohamad Rosli

Reactor Technology Centre, Malaysian Nuclear Agency
*Corresponding author: m_hairie@nm.gov.my

ABSTRACT

This study aims to predict the source term and decay heat of highly burned-up fuel from the RTP TRIGA reactor, a critical factor for ensuring safe handling and disposal. Data on the reactor's operational history and accumulated burnup were collected and analyzed. Burnup calculations were carried out using the TRIGLAV code, while nuclide inventory simulations were performed with the MCNPX code. The decay heat was also evaluated using MCNPX. The gamma radiation strength for a core case and the decay heat resulting from energy deposition within the spent fuel pool were assessed. Additionally, the conservative maximum source term for a single fuel element was determined, highlighting the contribution of gamma radiation from radionuclides to decay heat in surrounding materials. This study provides vital data on the source term and decay heat, supporting the safe management of spent fuel from the TRIGA reactor.

Keywords: Decay Heat, TRIGA Fuel, Sourceterm, MCNPX, TRIGLAV

INTRODUCTION

PUSPATI TRIGA Reactor

The Malaysian PUSPATI TRIGA Reactor (RTP), located at the Malaysian Nuclear Agency, achieved its first criticality on 28 June 1982 and remains the nation's only research reactor. Operating at a maximum thermal power of 1 MW, the reactor generates a neutron flux of up to 10^{13} $n \cdot cm^{-2} \cdot s^{-1}$, supporting applications in neutron activation analysis, isotope production, and reactor physics experiments. Its core utilizes U-ZrH fuel, known for its inherent safety characteristics, with a mixed configuration of three types of fuel elements, each with varying uranium weight percentages to support different operational and research needs. Since its initial operation, the RTP core has undergone 16 reshufflings to address fuel depletion and burnup (Rabir et al., 2022).

The latest core configuration, Core-16, is depicted in Figure 1. It features an annular core surrounded by a graphite reflector and cooled via natural convection. The core's seven concentric rings of fuel elements are interspersed with water, serving as both coolant and moderator. Core-16 comprises fuel elements of 8.5 wt.%, 12 wt.%, and 20 wt.% UZrH1.6 with 20% U-235 enrichment, along with four control rods, graphite elements, and a central thimble. Fuel dimensions are detailed in Figure 2. RTP employs four boron carbide control rods, three of which are fuel follower types, containing 8.5 wt.% UZrH1.6 and a B4C absorber above the fuel section, while the fourth is an air follower (Rabir et al., 2022).

The TRIGA reactor, with an estimated operational lifespan of 50 to 60 years, has seen the PUSPATI TRIGA Reactor already surpass 40 years of service (IAEA, 2016). As RTP approaches the end of its operational life, the development of a decommissioning plan is actively underway to ensure a structured and safe process. Key future decommissioning activities will include facility dismantling and spent fuel management, both of which require meticulous planning and execution. Initial preparatory efforts for spent fuel management are already in progress, focusing on the design and fabrication of a fuel transfer cask (FTC) and the design, construction, and commissioning of a spent fuel pool (SFP) facility. Additionally, the implementation of an ageing management program is critical to maintain safety and ensure operational reliability throughout the reactor's remaining years (IAEA, 2014).

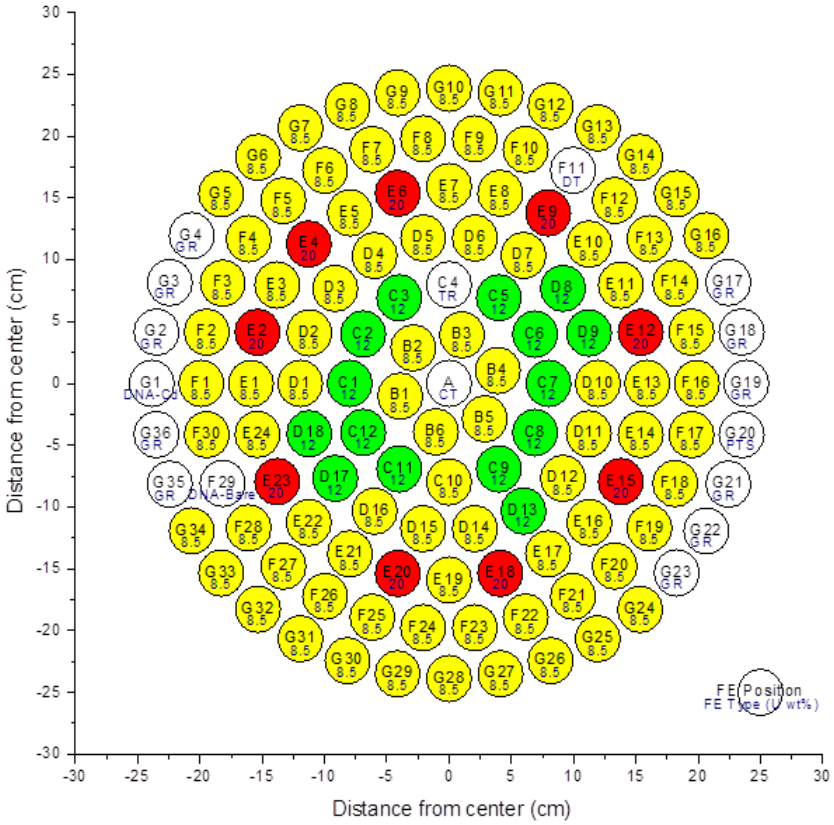

Figure 1: RTP's 16th core configuration featuring three types of fuel elements: 8.5 U wt. % (yellow), 12 U wt. % (green), and 20 U wt. % (red).

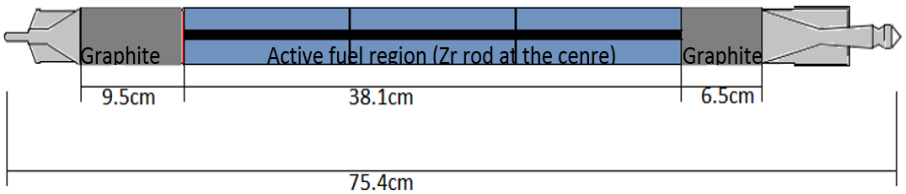

Figure 2: RTP fuel dimension

Importance of the subject

A comprehensive plan for managing highly burned-up research reactor fuel is critical to ensuring safety and compliance with regulatory requirements. The effective handling of such fuel demands meticulous preparation and the systematic collection of all relevant data. This includes detailed characterization of the fuel, focusing on parameters such as burnup, radionuclide inventory, and source-term determination. Understanding the source term is particularly important as it directly influences radiation safety measures, including shielding design and occupational exposure limits. Additionally, accurate source-term data enable precise modeling of radiological hazards during transport, storage, and eventual disposal, ensuring the protection of workers, the public, and the environment (El Maliki El Hlaibi et al., 2023).

Another crucial aspect to consider is the potential decay heat generated by the spent fuel and its impact on the surrounding structures within the storage facility. Decay heat can lead to thermal stress and material degradation, affecting the structural integrity of storage systems over time. Therefore, thermal analysis of the storage environment, including the interaction between the fuel and its containment, must be performed. This ensures that the facility design accommodates both immediate and long-term thermal loads, maintaining safe conditions throughout the storage period. By addressing these factors, the plan will provide a robust framework for the safe and sustainable management of highly burned-up research reactor fuel (Rochman et al., 2024).

Aim of study

The heat generated by the radioactive decay of fission products, known as radiation decay heat, is a critical factor to consider after a reactor shutdown. To support ongoing efforts in characterizing TRIGA reactor fuel for future handling procedure, this study focuses on evaluating decay heat with the following objectives: (1) To determine the radiation source term for the entire current RTP fuel inventory at its current burnup levels and for a single fuel element under extreme theoretical burnup conditions, (2) To identify the maximum radiation source term of an individual TRIGA fuel element, (3) To assess energy deposition due to decay heat within the SFP and the FTC.

The primary concern regarding decay heat lies in its long-term impact on structural integrity rather than immediate effects leading to incidents or accidents. In emergency scenarios, such as an accidental loss of coolant from the reactor pool, natural convection of air effectively removes fission product decay heat. This mechanism is sufficient to maintain fuel temperatures below critical levels, provided decay heat production is minimal or sufficient time has elapsed since reactor shutdown. Analytical results indicate that standard TRIGA fuel can tolerate temperatures up to 900°C without compromising cladding integrity. Furthermore, under coolant loss conditions, these thresholds are not surpassed if the thermal power per fuel element remains below 21 kW, ensuring structural safety (IAEA, n.d.).

METHODS

SFP design

As part of the RTP facility, SFP and FTC were constructed to support the future handling of spent or irradiated fuel. Concrete plays a critical role as a shielding material within the fuel pit facility and as shielding blocks. These materials were modeled and analyzed using MCNPX simulations to account for the decay heat generated by gamma radiation emitted from the fuel. The basic design of the SFP is illustrated in Figure 3. It consists of three fuel racks submerged in water at a depth of 4.5 meters and a width of 4.5 meters. All irradiated fuel is assumed to be loaded within these racks. In the MCNPX model, the SFP is divided into seven sections labeled A, B, C, D, E, F, G, along with a stainless-steel lining. Each section is assigned increasing neutron importance values (indicated by color coding) to enhance statistical accuracy as gamma radiation propagates farther from the source (fuel racks). Figure 4 displays the neutron importance values on the left and the corresponding section volumes on the right.

FTC design

The design of the Fuel Transfer Cask (FTC), shown in Figure 5, represents a standard configuration commonly utilized in TRIGA reactor facilities. The MCNPX model incorporates detailed material specifications, such as lead filling and a stainless-steel frame/wall, along with precise dimensional data. However, for the F6 tally, only the volume within the axial height of the fuel is considered. The FTC's radial model is segmented into radial sections (see Figure 6), following a similar methodology to the neutron importance assignments used for the SFP. This segmentation, based on varying neutron importance, enhances simulation accuracy. Additionally, dividing the model into separate cell volumes simplifies the application of cell tallies, such as F6 or F4, during MCNPX simulations.

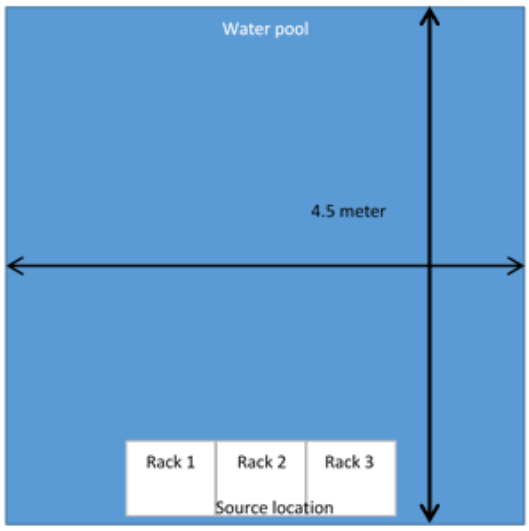

Figure 3: Basic design of SFP

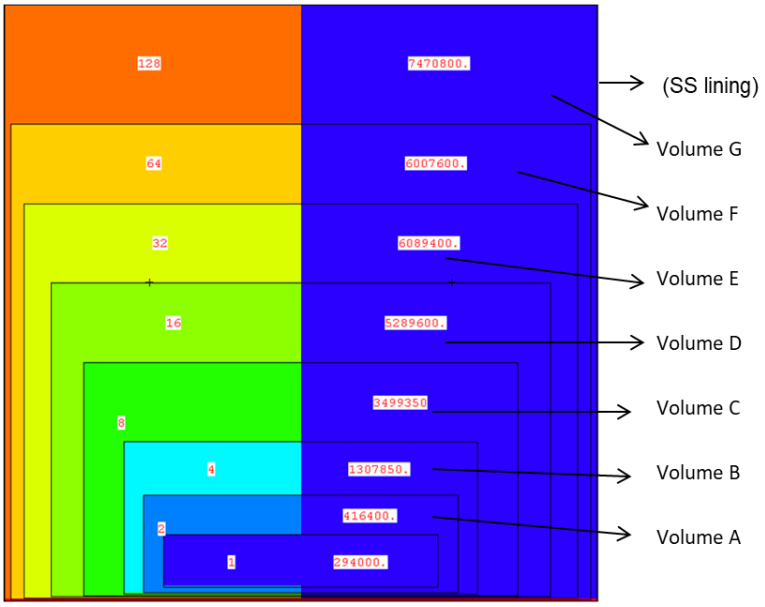

Figure 4: Sections in MCNPX model of the SFP

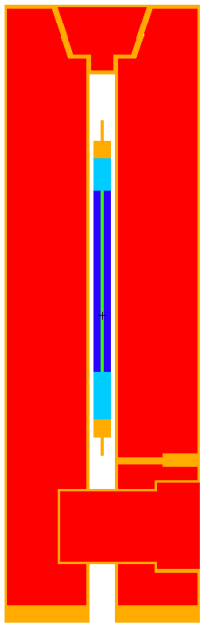

Figure 5: MCNPX model of TRIGA fuel inside FTC

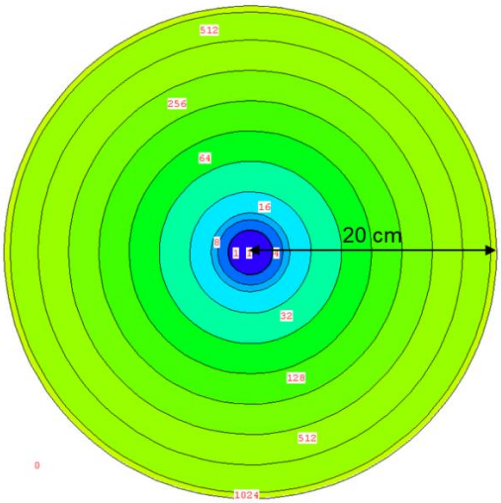

Figure 6: Radial sections in MCNPX model of the FTC

Simulation flow

The simulation process (see Figure 7) to estimate decay heat in the SFP begins with analyzing reactor operation history data, which provides key information on power levels and operating periods, forming the baseline for TRIGLAV calculations. From this, the core burnup is determined, and the burnup for individual fuel elements is obtained (Rabir et al., 2022). Using the calculated burnup, the radionuclide inventory is assessed via MCNPX's CINDER90 code, providing detailed information on the types and quantities of radioactive isotopes present in the spent fuel (Pelowitz, 2011) . Subsequently, the gamma radiation intensity and energy spectra emitted by the radionuclides in the fuel elements are evaluated. This data is then used in a separate MCNPX simulation to estimate the decay heat deposition within the SFP.

Additionally, a separate case was simulated to assess a single fuel element with the highest uranium content, conservatively assuming a burnup of up to 50%. The resulting radionuclide inventory and gamma radiation characteristics were determined before calculating its decay heat. To broaden the study's scope, simulations were also conducted to evaluate decay heat in the FTC, traditionally made of lead. Alternative materials, including normal concrete and high-density concrete, were also analyzed in separate simulations to explore their viability in decay heat management.

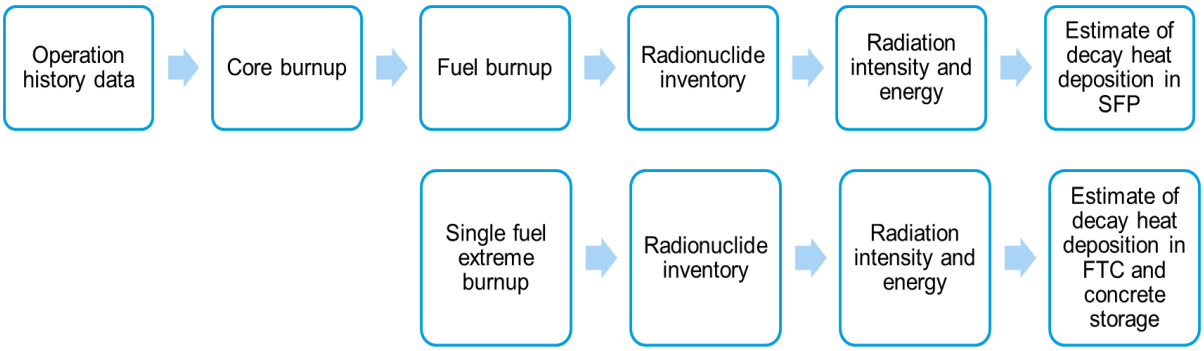

Figure 7: Simulation process flow for decay heat in the SFP (top) and the FTC with concrete shielding (bottom).

Operational data collection

Figure 8 illustrates the accumulation of burnup (measured in MWdays) over time, starting in February 1982 and projected into the 2030s. As of now, the RTP has accumulated approximately 800 to 850 MWdays of burnup, based on data retrieved from the RTP operational database. This burnup data is essential for TRIGLAV calculations, which provide a detailed record of fuel usage, and for MCNPX simulations, which predict the fission product inventory over the reactor's operational lifetime.

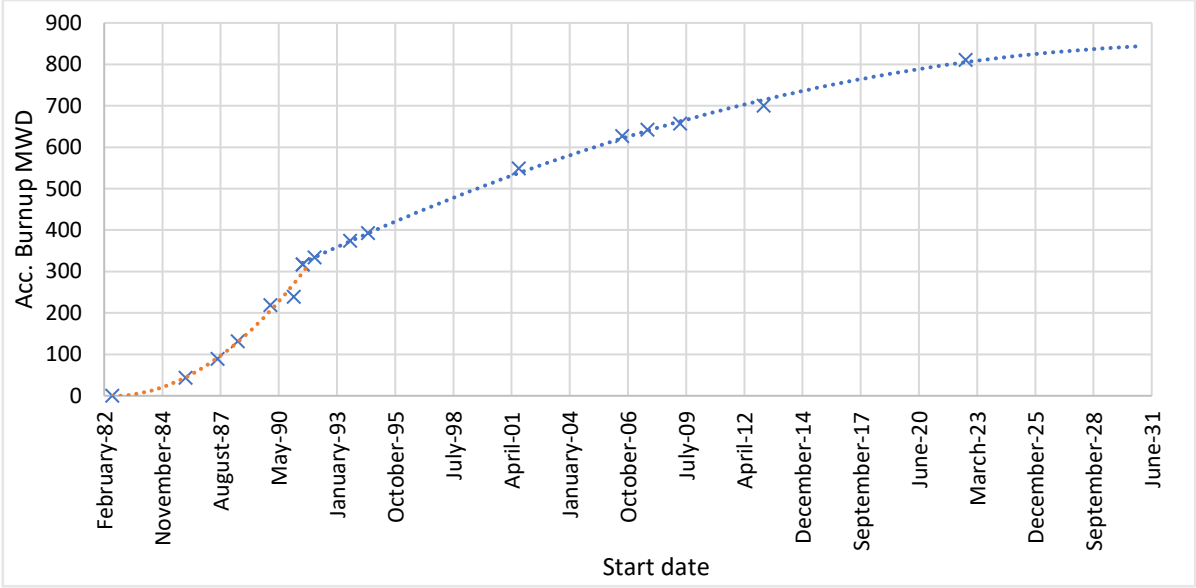

Figure 8: RTP accumulated total burnup

TRIGLAV burnup calculation

TRIGLAV is a deterministic code based on the diffusion approximation of the transport equation that employs the WIMSD program to calculate an averaged unit cell cross section. Core and individual fuel element burnup will be determined using the TRIGAV code (Rabir et al., 2022). As depicted in Figure 9, each fuel element (FE) will have a distinct burnup value due to its initial composition, loading history, and location within the core (Pungerčič et al., 2020).

TRIGLAV was selected for burnup calculations due to its validation for TRIGA reactors, computational efficiency, compatibility with RTP's operational data, and its successful integration with MCNPX for nuclide inventory and decay heat simulations. Compared to Monte Carlo-based alternatives like SERPENT or MCNPX-BURN, TRIGLAV offers a faster and deterministic approach, making it suitable for large-scale parametric studies.

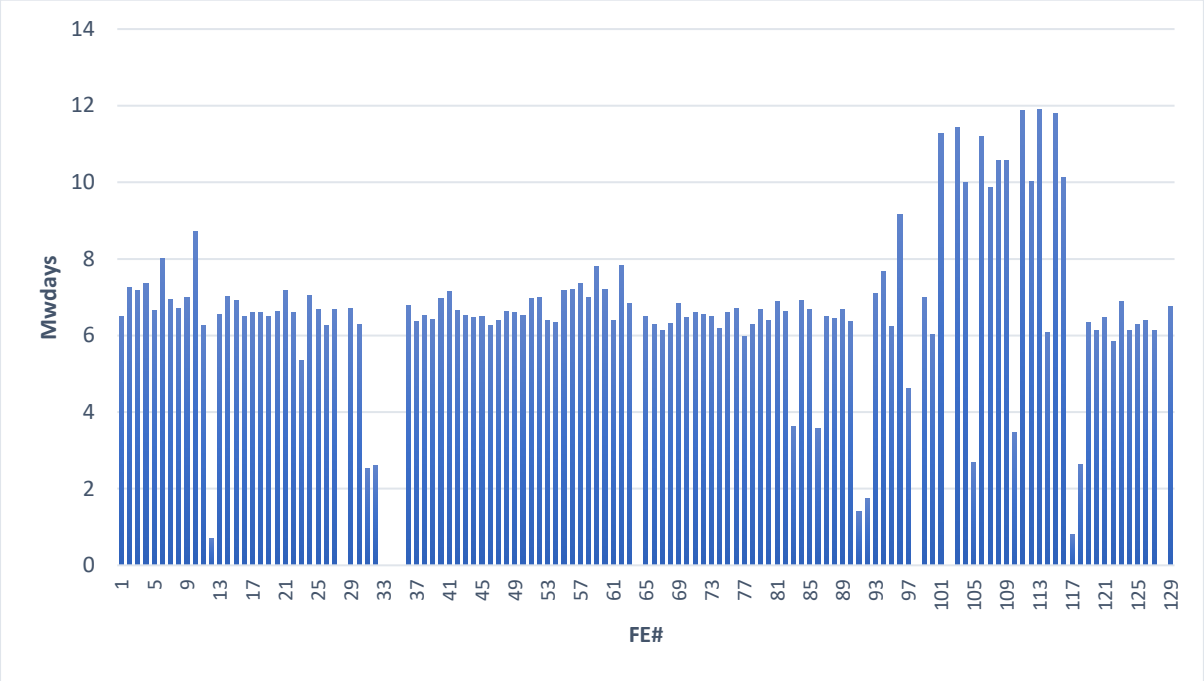

Figure 9: RTP individual fuel burnup values in MWdays, with each fuel element assigned a unit number up to #129.

Burnup and nuclide inventory simulation using MCNPX

The MCNPX code will be utilized to generate the nuclide inventory of each FE based on the burnup calculation from the TRIGLAV code. In the end, MCNPX fuel and core model of RTP Core-16 is developed using the nuclide inventories obtained previously. TRIGLAV generates burnup data for each RTP fuel element in units of MWdays, and this value is used as input in the MCNPX model. MCNPX performs burnup simulations and calculates the formation of actinides, fission products, and activation products in the RTP fuel for each different burnup value. This simulation is carried out using the 'BURN' card, where CINDER90 computes depletion, decay, and tracks all radionuclide changes in the model. Subsequently, the radiation emitted by radionuclides in the fuel is determined based on available published nuclide databases. This study focuses exclusively on gamma radiation to evaluate decay heat impacting materials surrounding the fuel. For scenarios involving extreme single-fuel burnup, MCNPX is directly utilized to simulate the theoretical burning of the selected fuel type until 50% of its fissile material is depleted, bypassing the use of MWdays as a reference.

After determining the gamma energy distribution and intensity, the F6 tally was employed to model decay heat. The F6 tally in MCNP calculates energy deposition within a material, which helps assess the dose or heating resulting from radiation interactions. It measures the energy deposited per unit mass (e.g., MeV/g) due to particle interactions within a specified cell. The tally output, measured in units of MeV/g, can then be directly converted into Watt-seconds (W·s) by applying the appropriate conversion factor. This energy value is scaled using both the mass of the fuel meat and the actual gamma intensity from the fuel, which was determined earlier in the analysis [7].

RESULTS AND DISCUSSION

Radionuclide inventory

MCNPX generates detailed radionuclide inventories, including buildup and decay following the cessation of fission, for each of the irradiated (from the total 129) fuel elements. Figures 10 and 11 present the actinide and non-actinide fission product inventories for a representative fuel element (FE#109). The inventories for other fuel elements exhibit similar trends, with variations in radionuclide magnitudes corresponding to differences in burnup values.

The actinides with the highest mass, aside from U-238 and U-235, include U-236 and Pu-239, as illustrated in Figure 10. In TRIGA fuel, the most significant actinides are U-236 and Pu-239. U-236 is primarily formed when U-235 captures a neutron without undergoing fission, although most of the U-236 nuclei eventually undergo fission to achieve stability. In contrast, Pu-239 is generated through the transmutation of U-238. This process involves neutron absorption by U-238, converting it to U-239, which then undergoes beta decay to form Np-239, followed by further beta decay to produce Pu-239.

The majority of the gamma radiation in spent fuel originates from the radioactive decay of these fission products, which include elements like Cs-137. The fission products inventory, as shown in Figure 11, includes several elements at the top, notably the isotopes of Xenon, Cesium, Neodymium, Promethium, Technetium, and Samarium. The selected nuclides are ranked based on their contribution to decay heat, which is a critical factor in post-irradiation fuel management. Cs-137 and Cs-134 are the dominant sources of medium- and short-term decay heat, respectively, due to their high fission yields and beta decay energies. Pm-147 also contributes significantly to early decay heat, particularly within the first few years after shutdown. I-127 and its decay product Xe-135 play a vital role in the initial hours to days, affecting both decay heat and reactivity control. While Sm-149 is not a major heat emitter, it is included due to its buildup from short-lived precursors and its strong neutron absorption that indirectly influences reactor cooldown behavior. Tc-99, though contributing minimally to decay heat, is considered for its long-term radiological impact and relevance in waste disposal. This ranking supports a more focused assessment of thermal behavior in spent fuel systems.

Gamma energy spectrum and intensity

MCNPX provides radionuclide data, including mass and activity in curies, which can be used to estimate radiation intensity. The energy and yield of each emitted radiation are derived from established published databases. Using this approach, all gamma energies and their intensities for the burned fuel elements were compiled, as summarized in Table 1.

This data can be evaluated for any specified decay time. For this analysis, a decay period of one year was chosen as a conservative baseline, aligning with the common practice of cooling and decaying fuel for at least 10 years before transfer to the SFP during the decommissioning process.

After one year of decay, specific gamma energies dominate the decay heat contribution. Among these, the 661.66 keV gamma radiation is the most significant, accounting for 8.13×10^{13} gamma/s or 61.1% of the total emitted gamma radiation. For the single fuel case, a similar trend was observed in the radionuclide species and gamma energy distribution, albeit with significantly lower magnitudes. This is illustrated in Figures 12 and 13. It is important to note

that gamma energies with fractions of 1×10^{-9} or lower were excluded from the analysis across all cases.

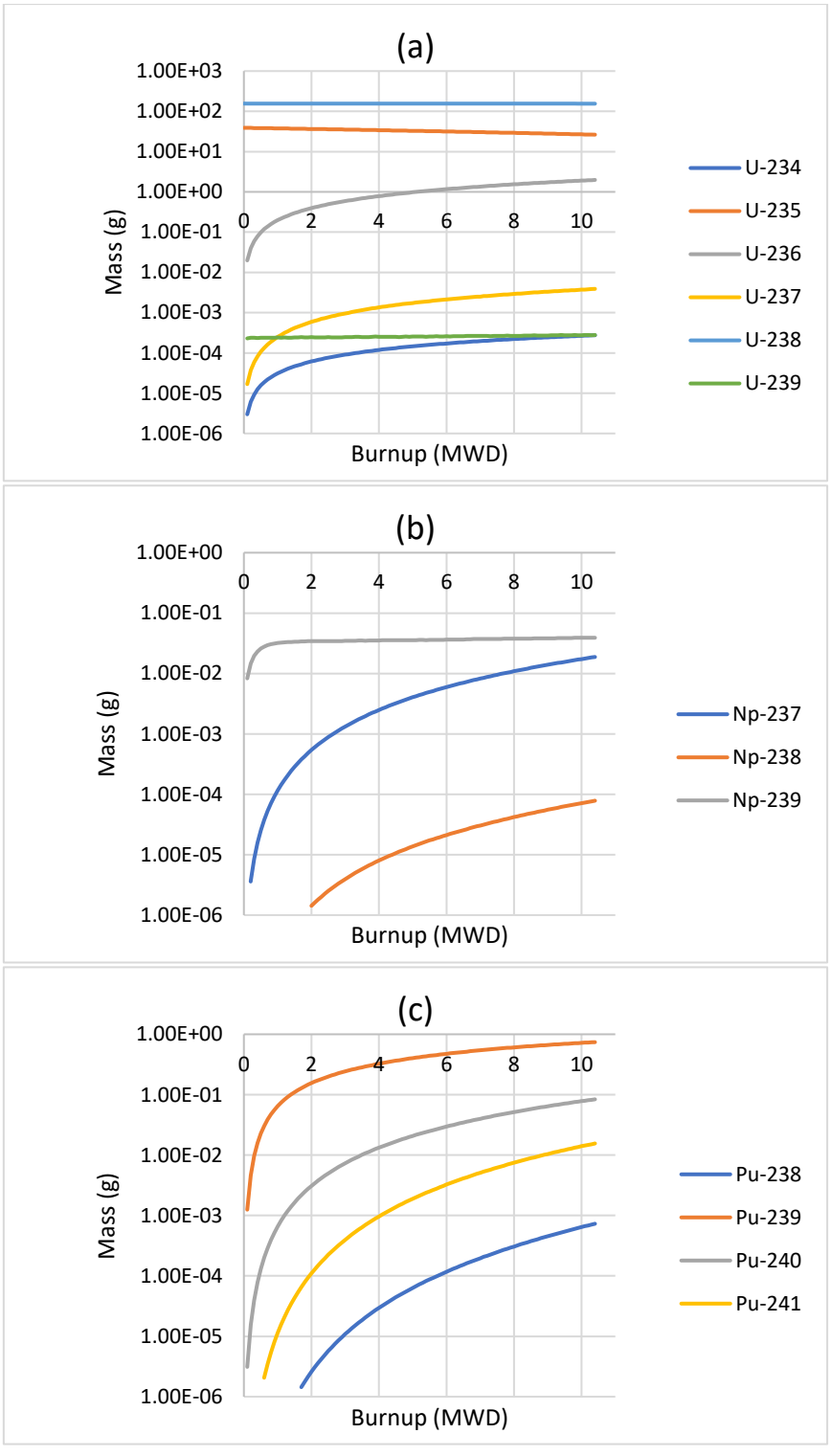

Figure 10: Isotopic inventory of major actinides in fuel element #109, showing Uranium (a), Neptunium (b), and Plutonium (c) isotopes.

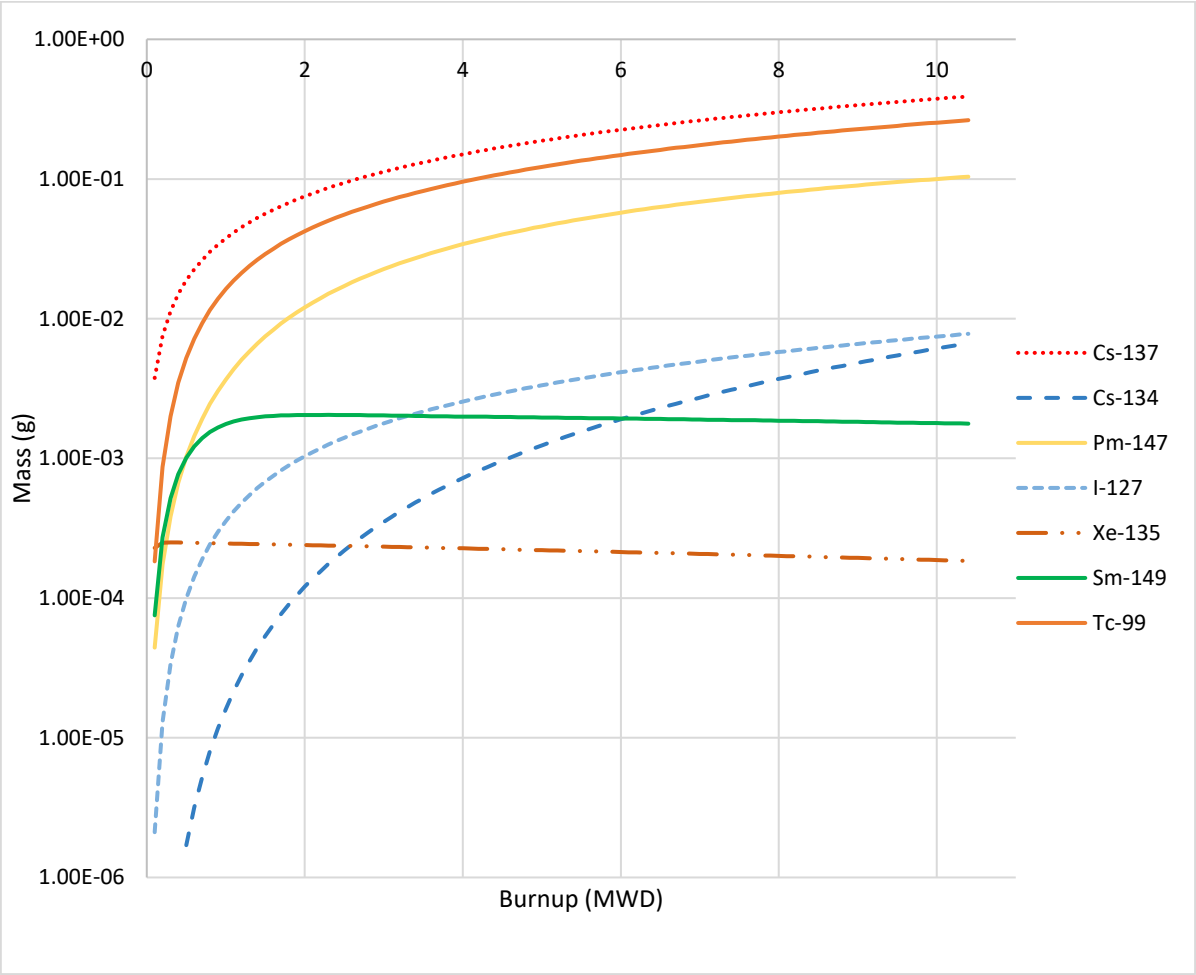

Figure 11: Major fission products inventory in fuel number #109

Table 1: Total RTP fuel's gamma energy and strength after 1-year decay

Gamma energy (KeV)	Gamma/second	Fraction
21.54	1.61E+08	1.21E-06
29.97	5.62E+05	4.23E-09
40.98	1.49E+11	1.12E-03
45.3	1.75E+09	1.32E-05
57.63	2.19E+10	1.65E-04
64.28	1.22E+06	9.17E-09
80.12	7.81E+11	5.87E-03
86.55	4.10E+10	3.08E-04
86.94	1.13E+06	8.50E-09
87.57	4.71E+06	3.54E-08
105.31	2.82E+10	2.12E-04
105.5	1.18E+08	8.87E-07
123.07	7.44E+08	5.59E-06
133.51	6.36E+12	4.78E-02
145.44	1.91E+11	1.44E-03
162.66	2.48E+05	1.86E-09
204.1161	4.07E+07	3.06E-07
235.69	3.51E+10	2.64E-04
427.87	1.25E+12	9.40E-03
484.471	4.05E+07	3.05E-07
497.08	6.44E+12	4.84E-02
537.26	9.72E+05	7.31E-09
550.27	6.75E+10	5.08E-04
556.65	1.01E+08	7.59E-07
557.06	5.94E+10	4.47E-04
561.9	2.18E+07	1.64E-07
569.33	1.66E+12	1.25E-02
600.6	7.48E+11	5.62E-03
604.72	1.05E+13	7.89E-02
610.33	4.08E+11	3.07E-03
629.97	6.33E+10	4.76E-04
635.95	4.75E+11	3.57E-03
661.66	8.13E+13	6.11E-01
695.88	2.61E+09	1.96E-05
723.3	3.69E+08	2.77E-06
724.19	5.76E+12	4.33E-02
725.7	2.34E+10	1.76E-04
729.57	5.89E+08	4.43E-06
756.73	7.07E+12	5.32E-02
765.803	1.45E+11	1.09E-03
795.86	9.23E+12	6.94E-02
908.96	3.68E+08	2.77E-06
933.838	2.79E+08	2.10E-06
1088.64	6.90E+07	5.19E-07
1204.77	2.06E+10	1.55E-04
1274.43	6.41E+08	4.82E-06
Total intensity	1.33E+14	1.00E+00

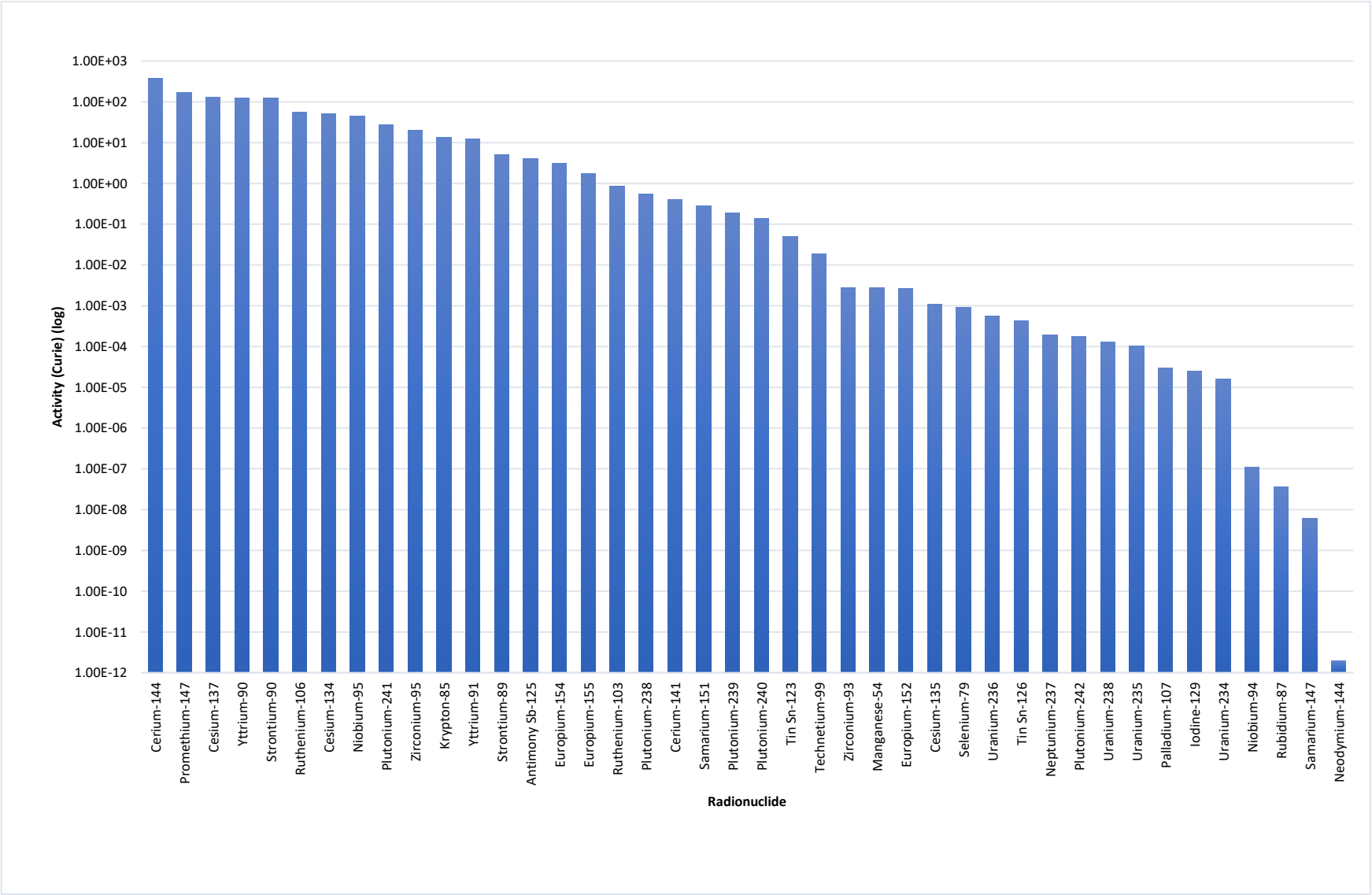

Figure 12: Fission product inventory for a single 20 wt% fuel rod at 50% burnup after 1-year cooling period.

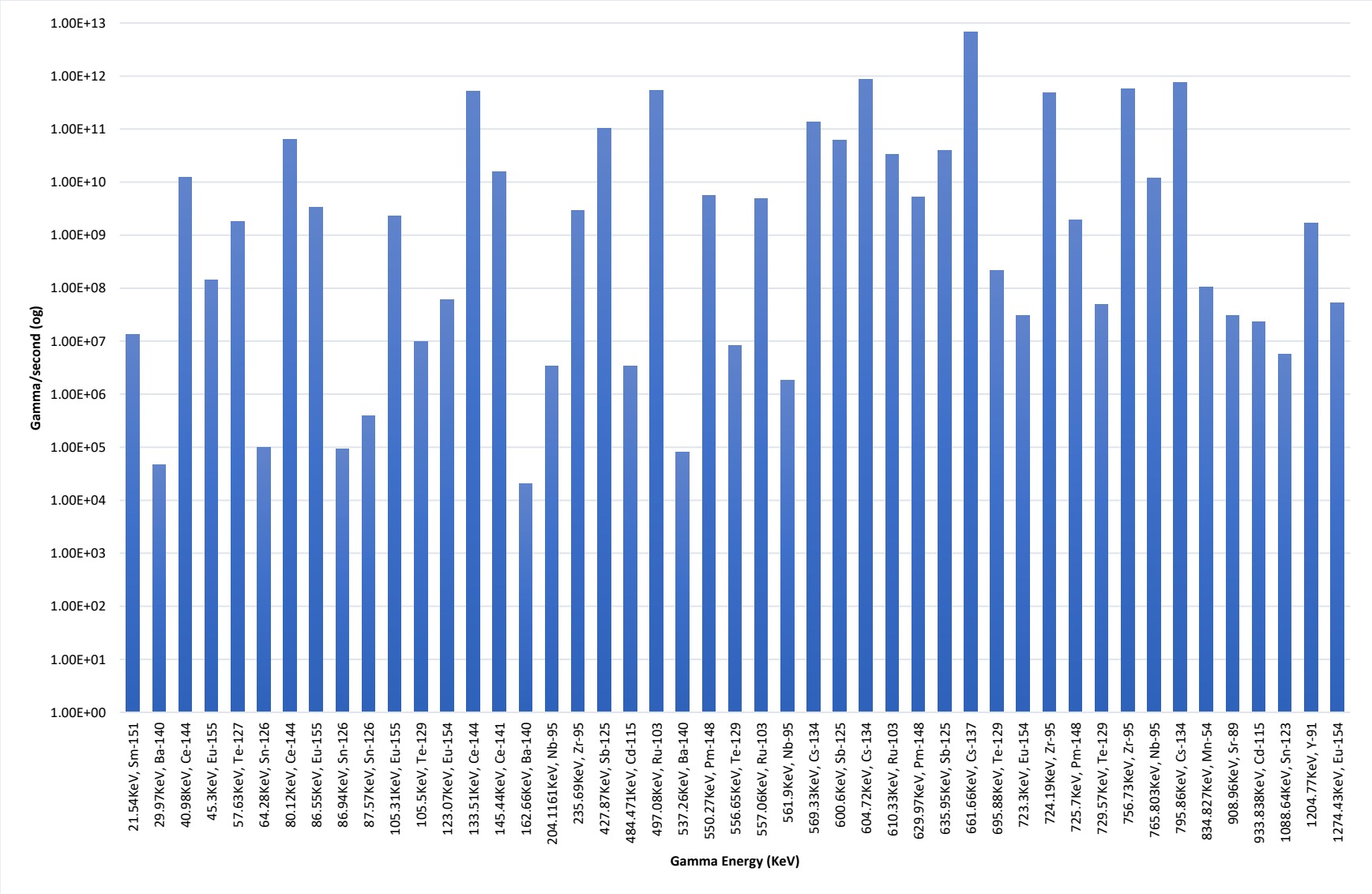

Figure 13: Gamma energy distribution and major intensities for a single 20 wt% fuel rod at 50% burnup after a 1-year cooling period.

Determination of decay heat in SFP

Gamma radiation propagates from the source at the bottom of the SFP, traveling in all directions through the water medium, before being absorbed by the stainless-steel lining. As the gamma radiation travels, part of its energy is absorbed by the surrounding materials, resulting in energy deposition. Since gamma radiation is more effectively absorbed by high-density materials, areas with higher density exhibit greater energy deposition, leading to higher decay heat (Ihsani et al., 2024). This phenomenon is illustrated in Figure 14, where decay heat decreases progressively with increasing distance from the source. However, the stainless-steel lining, being of higher density than water, may exhibit slightly higher decay heat compared to closer segments (e.g., volumes E, F, and G) due to its superior energy absorption properties. The density of stainless steel allows for more efficient gamma energy absorption and deposition, contributing to this localized increase in decay heat. Additionally, the gamma source is supported by the fuel rack, which is constructed from stainless steel within the SFP. As a result, the fuel rack is expected to experience the highest decay heat compared to all other volume segments. However, the analysis of the rack's thermal response and mass load will be addressed in future work.

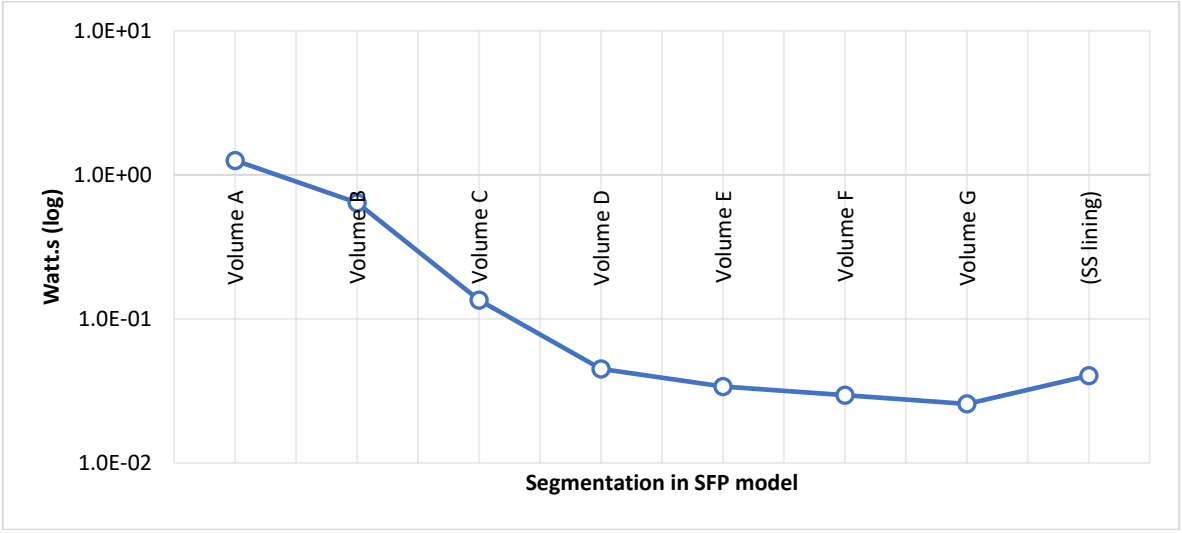

Figure 14: Total decay heat generated in each volume segment of the SFP model.

Determination of decay heat in FTC (lead) and in concrete

Figure 15 illustrates the decay heat trends for three different materials: lead (~11 g/cc), normal concrete (2.3 g/cc), and high-density concrete (3.4 g/cc). The maximum decay heat occurs in the innermost layer of the lead shield in the FTC, where it exponentially decreases with increasing distance from the source. In contrast, concrete materials, having lower density, allow more gamma radiation to pass through and deposit energy at greater distances from the inner layer. As a result, within the first 2 cm of thickness, concrete exhibits lower decay heat compared to lead (Bakos, 2006). However, as the distance increases, the decay heat in concrete does not decrease as rapidly as it does in lead, due to the lower energy absorption efficiency of concrete.

This phenomenon also applies to variations in density within the same material, such as concrete. In this case, high-density concrete exhibits higher decay heat than normal concrete

within the first 8 cm. Beyond 9 cm, the decay heat in normal concrete surpasses that of high-density concrete, and the two curves diverge further as the distance increases.

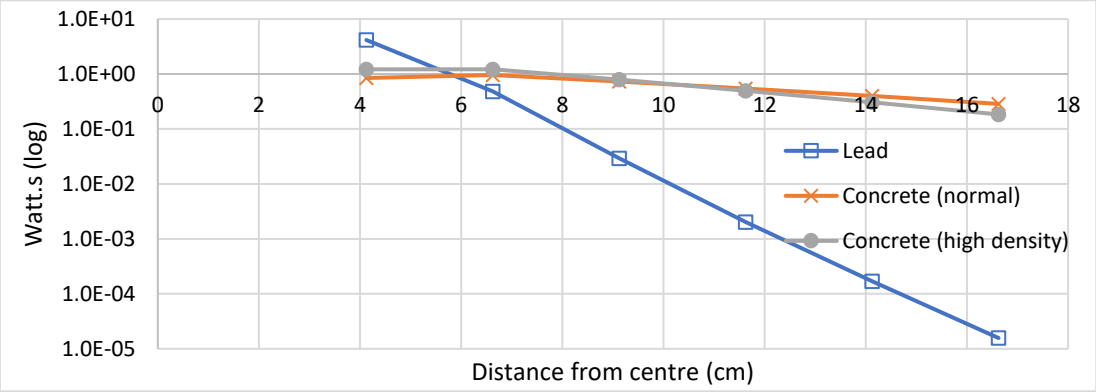

Figure 15: Decay heat variation as a function of distance for different materials in the single fuel case.

CONCLUSIONS

In conclusion, this study evaluates the radiation decay heat from TRIGA reactor fuel to aid in future handling procedures. It successfully determines the radiation source term for the current RTP fuel inventory and individual fuel elements under extreme burnup conditions. Additionally, the study assesses the energy deposition from decay heat within both the SFP and FTC. The simulation process for estimating decay heat in the SFP starts with reactor operation history data, which informs TRIGLAV calculations and determines the core burnup and individual fuel element burnup. Using the calculated burnup, the radionuclide inventory is assessed with the MCNPX CINDER90 code, and gamma radiation intensity and energy spectra are evaluated to estimate decay heat.

The detailed radionuclide inventory generated by MCNPX provides a comprehensive understanding of the isotopes present in irradiated TRIGA fuel elements, including their buildup and decay over time. Actinides such as U-236 and Pu-239 are identified as significant contributors to the fuel's composition, with the majority of gamma radiation arising from the decay of fission products like iodine-131 and cesium-137. The gamma energy spectrum, compiled from established databases, reveals that after one year of decay, the 661.66 keV gamma radiation is the most prominent, accounting for a substantial portion of the total emitted gamma radiation.

The gamma radiation is absorbed more effectively by higher-density materials, such as the stainless-steel lining, leading to increased decay heat compared to surrounding segments. Lead exhibits the highest decay heat near the source, with heat decreasing exponentially as distance increases, while concrete allows more gamma radiation to penetrate, resulting in lower decay heat initially but a slower decrease over distance.

A detailed analysis and simulation are currently underway to further investigate the properties of the source term, including the effects of axial burnup distribution. Additionally in the future, the study aims to explore various structural configurations and materials within the defined scope.

ACKNOWLEDGEMENTS

The author would like to express gratitude to the Reactor Technology Centre of the Malaysian Nuclear Agency for their support of this study.

REFERENCES

Bakos, G. C. (2006). Calculation of γ radiation converted to thermal energy in nuclear reactor shielding facilities. *Annals of Nuclear Energy*, *33*(3), 236–241.

El Maliki El Hlaibi, S., Lamkaddam, O., El Bardouni, T., Chakri, A., & Misdaq, M. A. (2023). Calculation of the activity inventory of the CENM TRIGA MARK II reactor for decommissioning planninig. *Radiation Physics and Chemistry*, *207*, 110837.

IAEA. (2014). *Project Experiences in Research Reactor Ageing Management, Modernization and Refurbishment*.

IAEA. (2016). *History, Development and Future of TRIGA Research Reactors* (No. 482). Vienna, Austria: IAEA

IAEA. (n.d.). TRIGA REACTOR CHARACTERISTICS. Retrieved from https://ansn.iaea.org/Common/documents/Training/TRIGA Reactors (Safety and Technology)/pdf/chapter1.pdf

Ihsani, R. N., Gareso, P. L., & Tahir, D. (2024). An overview of gamma radiation shielding: Enhancements through polymer-lead (Pb) composite materials. *Radiation Physics and Chemistry*, *218*, 111619.

Pelowitz, D. B. (2011). *MCNPX TM User's manual version 2.7.0*. Los Alamos, NM, USA: Los Alamos Scientific Laboratory.

Pungerčič, A., Čalič, D., & Snoj, L. (2020). Computational burnup analysis of the TRIGA Mark II research reactor fuel. *Progress in Nuclear Energy*, *130*, 103536.

Rabir, M. H., Muttaqin, A., Bayar, J., & Karim, J. A. (2022). In-Core Rtp Fuel Relocation and Criticality Behaviour Using Mcnp5 / X Code. *Jurnal Nuklear dan Teknologi Relatif*, *19*(1), 8–18.

Rochman, D., Hursin, M., Pillon, S., St-Jean, C., Leconte, P., & Serot, O. (2024). An introduction to Spent Nuclear Fuel decay heat for Light Water Reactors: a review from the NEA WPNCS. *EPJ Nuclear Sciences & Technologies*, *10*, 9.